



Received November 10, 2020, accepted November 18, 2020, date of publication November 23, 2020, date of current version December 8, 2020.

Digital Object Identifier 10.1109/ACCESS.2020.3039783

# An Effective Method for Estimating State of Charge of Lithium-Ion Batteries Based on an Electrochemical Model and Nernst Equation

LIHUA LIU<sup>1</sup>, JIANGUO ZHU<sup>1</sup><sup>2</sup>, (Senior Member, IEEE),  
AND LINFENG ZHENG<sup>1,3,4</sup>, (Member, IEEE)

<sup>1</sup>Tianjin Key Laboratory of Advanced Electrical Engineering and Energy Technology, Tiangong University, Tianjin 300387, China

<sup>2</sup>School of Electrical and Information Engineering, The University of Sydney, Darlington, NSW 2006, Australia

<sup>3</sup>Institute of Rail Transportation, Jinan University, Zhuhai 519070, China

<sup>4</sup>International Energy College, Jinan University, Zhuhai 519070, China

Corresponding author: Linfeng Zheng (lfzheng@jnu.edu.cn)

This work was supported by the Guangdong Basic and Applied Basic Research Foundation under Grant 2019A1515012210.


**ABSTRACT** Lithium-ion batteries are generally regarded as a leading candidate for energy storage systems. The safe and reliable operation of lithium-ion batteries depends largely on accurate estimation of the state of charge (SOC), which requires an accurate battery model. Bearing strong mechanisms, the electrochemical model (EM) can mimic the battery dynamics with high fidelity, and thus the EM-based methods can produce more reliable SOC estimates. This paper proposes a novel EM-based SOC estimation method for lithium-ion batteries from the electrochemical mechanism perspective. Firstly, a single particle model is employed to gain a direct insight into the electrochemical reactions inside the battery, and it is found that the model output voltage and SOC are strongly related to the lithium-ion concentrations of solid phases. A simple negative voltage feedback module is then applied to observe the voltage error between the cell referenced terminal voltage and the model output voltage. To eliminate the voltage error and achieve a precise estimate, a quantitative relationship between the voltage error and corrected amount of lithium-ion concentrations is deduced based on the Nernst equation. The performance of proposed method has been systemically evaluated under different operating conditions, including various charging and discharging current rates, erroneous initial SOC, and cell aging levels. Although an erroneous initial SOC of 50% is applied to the proposed algorithm, promising estimates with the mean absolute errors of 0.22% and 1.35% can be still achieved under the constant and dynamic loading conditions, respectively.

**INDEX TERMS** Lithium-ion battery, state of charge (SOC), electrochemical model, Nernst equation.

## I. INTRODUCTION

With numerous advantages, such as high energy density, low self-discharging rate, no memory effects, and long lifespan, and so on, lithium-ion batteries are generally regarded as a leading energy storage candidate for electric vehicles, renewable energy systems, portable electronic devices, and many other applications [1]–[3]. In most lithium-ion battery energy storage systems, a battery management system (BMS) is employed to manage the performance and maintain the longevity of battery cells [1], [4], [5]. The functions of

a BMS include mainly cell voltage detection and balancing [6], [7], estimation of state of charge (SOC) [8]–[11] and state of health (SOH) [12]–[14], and thermal management [15]–[18]. Defined as the ratio of the residual charge stored in a battery to its maximum available capacity, the SOC is one of the primary and critical parameters for the development of battery management strategies [19]. Accurate SOC estimation plays a vital role in controlling the safe charging and discharging of the battery while guaranteeing its efficiency. However, the SOC cannot be measured directly and accurately by sensors like ordinary physical quantities in practices. Despite the huge research efforts, the battery SOC estimation still poses a significant challenge

The associate editor coordinating the review of this manuscript and approving it for publication was Guijun Li<sup>1</sup>.

due to the complexity and nonlinearity of electrochemical reactions.

### A. REVIEW OF SOC ESTIMATION METHODS

According to whether the SOC estimations used for online applications or not, the SOC estimation methods can be divided into offline and online estimation methods. The offline estimation methods mainly include the open circuit voltage (OCV) [20], [21], electromotive force [22], internal resistance [23], and impedance spectroscopy [24]. Though generally simple and readily implementable, they have great strict requirements for experimental conditions and time. Because these methods need to interrupt normal operations of the battery, they are only suitable for measurement in laboratories or as a cross check for other estimation methods.

The online estimation methods mainly include the coulomb-counting (CC), computer intelligence methods, and model-based methods. The CC method computes the SOC by integrating the battery loading current over time, and requires an accurate initial SOC [4]. However, finding the accurate initial SOC itself is a challenge. Also, its estimates are susceptible to current drift and measurement noise.

The computer intelligence-based methods estimate the battery SOC by utilizing some intelligent algorithms, such as the genetic algorithm [25], particle swarm optimization [26], fuzzy logic [27], neural network [28], [29], and support vector machine [30], etc. Treating the battery as a black-box system, these methods approximate the relationship between the SOC and other variables by training the approximate model with a large quantity of experimental data. Promising accuracy can be achieved with reliable training data, but these methods may fail in unexpected training conditions.

The model-based SOC estimation methods have attracted considerable attentions due to their remarkable advantages of closed-loop control and insensitivity to unexpected disturbances. The reported model-based SOC estimation methods mainly differ from the battery models and observers employed in the methods [31]. Commonly used battery models include equivalent circuit models (ECMs) and electrochemical models (EMs). In the ECMs, the characteristics of circuit elements such as the voltage source, resistance, and capacitance are applied to simulate the battery dynamics. Simple and flexible model structure of the ECMs promotes their controllability and applicability in practices [19]. However, the ECMs fail to give the full expression to the battery dynamics due to the lack of the representations of physicochemical reactions inside the battery. Different from the ECMs, EMs are derived based on the electrochemical reaction mechanisms and thus have the capability to elaborate the battery dynamics, such as lithium-ion diffusion and intercalation/de-intercalation. Knowledge of these dynamics inside the battery significantly enables more reliable and accurate battery state estimation. The development of EMs with control algorithms, however, is severely hampered by their complexity.

The most frequently used observers in model-based SOC estimation methods include the H-infinity filter [32], derivative

Kalman filters [9], [10], particle filter [8], and sliding mode observer [33], [34]. While the use of these observers can improve the accuracy of the model and the SOC estimation, they bring extra complexity and computational efforts to the estimation algorithms. It is also worth mentioning that most of the observe parameters are usually determined by empirical knowledge and need to be calibrated by a tedious procedure, which is not associated with the mechanisms of electrochemical reaction inside the battery. Very few reports investigated observers from the perspective of electrochemical mechanisms to improve the performance of model-based methods. More efforts are therefore needed to address these issues.

### B. KEY CONTRIBUTIONS

To address the knowledge gaps mentioned above, a novel EM-based battery SOC estimation method is proposed in this paper, and the key contributions of this work are summarized as the following:

- 1) An approach from the perspective of electrochemical mechanisms is proposed for estimating lithium-ion battery SOC, based on a battery single particle model and the Nernst equation.
- 2) A simple voltage negative feedback is applied to eliminate the voltage error between the battery referenced terminal voltage and the model output voltage. The relationship between the voltage error and the corrected amount of lithium-ion concentrations in solid phase is quantitatively deduced by using the Nernst equation.
- 3) The robustness and effectiveness of the proposed SOC estimation method are systemically validated under different operating situations, including various charge/discharge current rates and cell aging levels, erroneous initial SOCs, and dynamic conditions.

### C. PAPER ORGANIZATION

The remainder of this paper is organized as follows. Section II introduces a simplified battery EM to depict the electrochemical reactions inside the battery. The proposed battery SOC estimation method based on the lithium-ion concentration and Nernst equation is presented in Section III. Section IV demonstrates the experimental results and discussions, followed by a summary of the main conclusions and future work in Section V.

## II. BATTERY ELECTROCHEMICAL MODEL

As shown in Fig. 1, the schematic of a typical battery EM, 1D-spatial model, consists of a porous negative electrode, a porous positive electrode, an electron-blocking separator, and electrolyte. When the lithium-ion battery is charging, lithium-ions de-intercalate from the positive electrode and pass through the separator to the negative electrode. The more lithium-ions intercalate to the negative electrode, the more energy is charged into the battery. On the contrary, during the battery discharging process, lithium-ions de-intercalate from

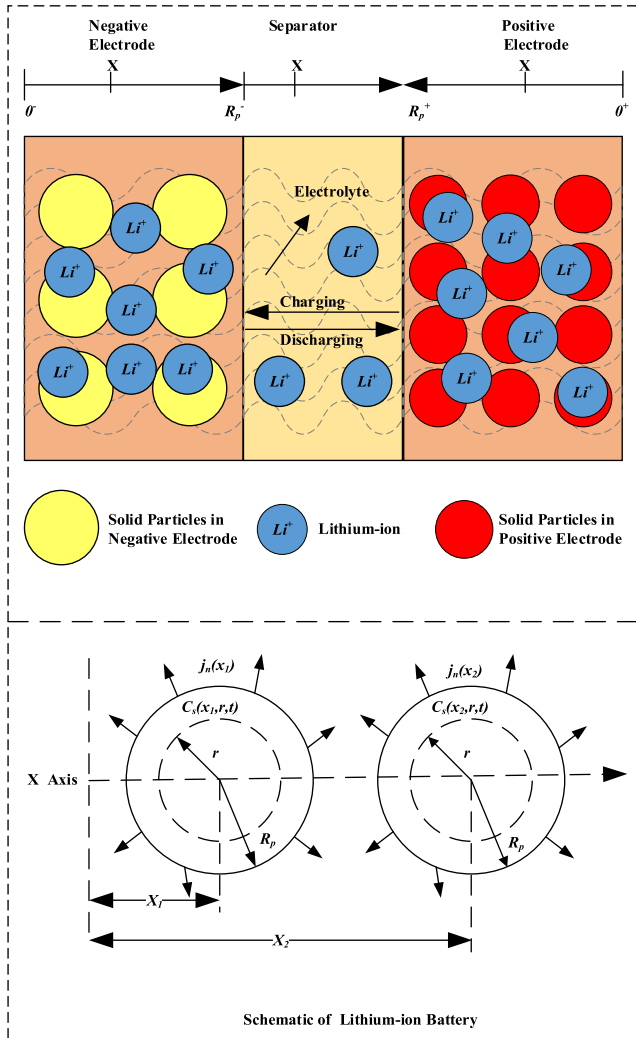


FIGURE 1. Schematic of a lithium-ion battery electrochemical model.

the negative electrode and then travel across the separator to the positive electrode.

In the model, the lattice structure of a lithium-ion battery electrode is visualized as small spherical solid particles that are assumed to be uniformly dispersed along the X-axis to hold lithium-ions in the solid phase [1], [4]. The intercalation and de-intercalation processes of lithium-ions are visualized by the ions moving in and out of the spherical solid particles. During the charging and discharging, the lithium-ions and charges in the positive and negative electrodes and liquid are conserved. Table 1 lists the governing equations for describing the dynamics of lithium-ion batteries. More details about the dynamics of lithium-ion batteries can be found in the literature [1], [4].

As listed in Table 1, the dynamics of lithium-ion batteries can be described by a set of partial differential equations (PDEs). These equations are difficult to apply directly in practice, especially for further development of advanced EM-based algorithms. To simplify the model, each electrode

TABLE 1. The dynamic behavior of Lithium-ion batteries.

Equation	Description
$\frac{\partial c_s(x, r, t)}{\partial t} = \frac{1}{r^2} \frac{\partial}{\partial r} (D_s r^2 \frac{\partial c_s(x, r, t)}{\partial r})$ (1)	Solid-phase lithium-ion diffusion
$\frac{\partial c_e(x, t)}{\partial t} = \frac{\partial}{\partial x} (D_e \frac{\partial c_e(x, t)}{\partial x}) + \frac{1}{F \epsilon_e} \frac{\partial (t_a^0 i_e(x, t))}{\partial x}$ (2)	Electrolyte-phase lithium-ion diffusion
$\frac{\partial i_e(x, t)}{\partial x} = a F j_n(x, t)$ (3)	Conservation of charge
$j_n(x, t) = \frac{i_0(x, t)}{F} \exp(\frac{a_a F}{RT} \eta_s(x, t)) - \frac{i_0(x, t)}{F} \exp(\frac{a_c F}{RT} \eta_s(x, t))$ (4)	Butler-Volmer kinetics
$\eta_s(x, t) = \Phi_s(x, t) - \Phi_e(x, t) - U(c_s(x, R_p, t)) - F R_f j_n(x, t)$ (5)	Solid-phase intercalation overpotential
$i_0(x, t) = r_{eff} c_e(x, t)^{\alpha_e} c_s(x, R_p, t)^{\alpha_s} \cdot (c_{s, max} - c_s(x, R_p, t))^{\alpha_s}$ (6)	Exchange current density

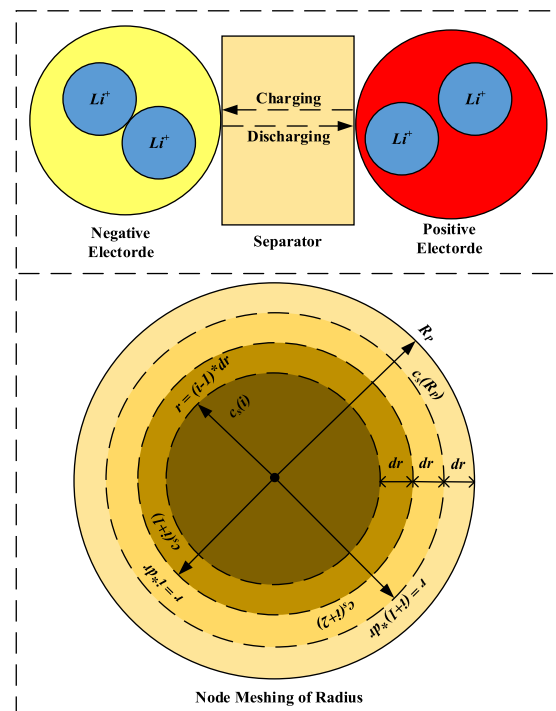


FIGURE 2. Schematic of SPM for Lithium-ion Battery.

of the battery can be visualized as a single spherical solid particle that holds the lithium-ions in each of its layers, as shown in Fig. 2. The simplified model is known as the single particle model (SPM). This approximation is also studied in the literature [1], [4].

In the SPM, the lithium-ion concentration in electrolyte is deemed to be uniform, namely

$$\frac{\partial c_e}{\partial t} = \frac{\partial c_e}{\partial x} = 0 \quad (7)$$

Thus, the SPM considers mainly the solid phase lithium-ion diffusion. The total number of lithium-ions and the mean lithium-ion concentration in the solid electrode can be determined by

$$n_{s\_total} = \int_0^{R_p} 4\pi r^2 c_s(r, t) dr \quad (8)$$

$$c_{s\_mean} = n_{s\_total} / \left( \frac{4}{3} \pi R_p^3 \right) \quad (9)$$

where  $n_{s\_total}$  and  $c_{s\_mean}$  denote the total number of lithium-ions and the mean lithium-ion concentration in the solid electrode, respectively.

Equations (8) and (9) can be further discretized as

$$n_{s\_total} = \sum_{i=2}^{n_1} c_s(i, k) 4\pi ((i-1)dr)^2 dr \quad (10)$$

$$c_{s\_mean} = \frac{3}{(n_1-1)^3} \sum_{i=2}^{n_1-1} (c_s(i, k)(i-1)^2) \quad (11)$$

The mean lithium-ion concentration in the electrode can be employed to compute the battery SOC by [1]

$$SOC = \frac{c_{s\_mean} - c_{s\_SOC=0\%}}{c_{s\_SOC=100\%} - c_{s\_SOC=0\%}} \quad (12)$$

The output voltage,  $U$ , of the SPM can be determined by

$$U(t) = \Phi_s(0^+, t) - \Phi_s(0^-, t) - I(t)R_c \quad (13)$$

where  $\Phi_s(0^+, t)$  and  $\Phi_s(0^-, t)$  denote the potentials of positive and negative electrodes, respectively, and  $R_c$  represents the empirical contact resistance of the battery.

The electrode potential,  $\varphi$ , of the battery can be calculated by

$$\varphi(t) = \Phi_s(0^+, t) - \Phi_s(0^-, t) \quad (14)$$

By substituting (14) into (13), the output voltage can be rewritten as

$$U(t) = \varphi(t) - I(t)R_c \quad (15)$$

By combining (1)-(7), the output voltage can be obtained as

$$\begin{cases} U(t) = \frac{2RT}{F} \ln \frac{y^+ + \sqrt{1 + (y^+)^2}}{-y^- + \sqrt{1 + (y^-)^2}} + I(t)R_{sum} \\ \quad + U^+(c_s(R_p^+, t)) - U^-(c_s(R_p^-, t)) \\ y^+ = \frac{I(t)}{2a^+L^+r_{eff}^+ \sqrt{c_e^+ c_s^+(R_p^+, t)(c_{s,max}^+ - c_s^+(R_p^+, t))}} \\ y^- = \frac{I(t)}{2a^-L^-r_{eff}^- \sqrt{c_e^- c_s^-(R_p^-, t)(c_{s,max}^- - c_s^-(R_p^-, t))}} \end{cases} \quad (16)$$

where  $c_s(R_p, t)$  and  $c_{s,max}$  denote the outermost lithium-ion concentration and the maximum lithium-ion concentration, respectively;  $R_{sum}$  is the sum of contact and SEI film resistances; and  $U(c_s(R_p, t))$  represents the open circuit potential of the electrode.

### III. THE PROPOSED SOC ESTIMATION METHOD

#### A. FEEDBACK VOLTAGE ERROR AND LITHIUM-ION CONCENTRATION CORRECTION

As shown in (12) and (16), the SOC and model output voltage are strongly related to the lithium-ion concentrations of solid phases. During the battery charging and discharging processes, the cell terminal voltage can be accurately measured by voltage sensors. A simple voltage negative feedback is employed to observe the voltage error between the referenced cell terminal voltage and model output voltage. It is necessary to eliminate the voltage error by correcting the lithium-ion concentrations to ensure that the model can precisely mimic the dynamics of lithium-ion battery, thus achieving an accurate SOC estimation.

Assume that at time instant  $t = k$ , there are errors between the estimated and actual values of the SOC and  $U$ , noted as  $\Delta SOC(k)$  and  $\Delta U(k)$ , respectively. For the purpose of eliminating the errors, an amount of correction of lithium-ion concentration is added at the time instant  $t = k + 1$ , and the revised lithium-ion concentration values can be calculated as

$$\begin{cases} c_s^{+*}(i, k+1) = c_s^+(i, k+1) + \Delta c_s^+(k+1) \\ c_s^{-*}(i, k+1) = c_s^-(i, k+1) + \Delta c_s^-(k+1) \end{cases} \quad (17)$$

where  $i = 2, 3, \dots, n_1$ ,  $k = 2, 3, \dots, n_2$ ;  $\Delta c_s^+(k+1)$  and  $\Delta c_s^-(k+1)$  denote the corrected amount of lithium-ion concentration for the positive electrode and the negative electrode at the time of ( $t=k+1$ ), respectively; and  $c_s^{+*}(i, k+1)$  and  $c_s^{-*}(i, k+1)$  represent the revised lithium-ion concentration in the positive electrode and the negative electrode at time instant  $k+1$ , respectively.

By substituting (17) into (11), the corrected mean lithium-ion concentration can be calculated by

$$\begin{aligned} c_{s\_mean}^{+*}(k+1) &= \frac{3}{(n_1-1)^3} \sum_{i=2}^{n_1} ((c_s^+(i, k+1) + \Delta c_s^+(k+1))(i-1)^2) \\ &= \frac{3}{(n_1-1)^3} \sum_{i=2}^{n_1-1} (c_s^+(i, k+1))(i-1)^2 \\ &\quad + \frac{3}{(n_1-1)^3} \sum_{i=2}^{n_1} (\Delta c_s^+(k+1))(i-1)^2 \\ &= c_{s\_mean}^+(k+1) + \frac{n_1(2n_1-1)}{2(n_1-1)^2} \Delta c_s^+(k+1) \\ &= c_{s\_mean}^+(k+1) + \Delta c_{s\_mean}^+(k+1) \end{aligned} \quad (18)$$

$$\begin{aligned} \Delta c_{s\_mean}^+(k+1) &= \frac{n_1(2n_1-1)}{2(n_1-1)^2} \Delta c_s^+(k+1) \end{aligned} \quad (19)$$

$$\begin{aligned} c_{s\_mean}^{-*}(k+1) &= c_{s\_mean}^-(k+1) + \Delta c_{s\_mean}^-(k+1) \end{aligned} \quad (20)$$

$$\begin{aligned} \Delta c_{s\_mean}^-(k+1) &= \frac{n_1(2n_1-1)}{2(n_1-1)^2} \Delta c_s^-(k+1) \end{aligned} \quad (21)$$

where  $\Delta c_{s\_mean}^{+*}(k + 1)$  and  $\Delta c_{s\_mean}^{-*}(k + 1)$  denote the revised mean lithium-ion concentration in the positive and the negative electrodes at time instant  $k + 1$ , respectively;  $\Delta c_{s\_mean}^{+}(k + 1)$  and  $\Delta c_{s\_mean}^{-}(k + 1)$  denote the corrected amount of mean lithium-ion concentrations in the positive and negative electrodes at time instant  $k + 1$ , respectively.

Based on (12), the battery SOC can be calculated by using the lithium-ion concentrations of positive and negative electrodes, respectively, as

$$SOC^{+} = \frac{c_{s\_mean}^{+} - c_{s\_SOC=0\%}^{+}}{c_{s\_SOC=100\%}^{+} - c_{s\_SOC=0\%}^{+}} \quad (22)$$

$$SOC^{-} = \frac{c_{s\_mean}^{-} - c_{s\_SOC=0\%}^{-}}{c_{s\_SOC=100\%}^{-} - c_{s\_SOC=0\%}^{-}} \quad (23)$$

The SOC<sub>s</sub> calculated by (19) and (20) should be equal, namely

$$SOC^{+} = SOC^{-} \quad (24)$$

By substituting (22) and (23) into (24), the relationship between the mean lithium-ion concentrations of positive and negative electrodes can be obtained as

$$\begin{cases} c_{s\_mean}^{+} = \frac{c_{s\_SOC=100\%}^{+} - c_{s\_SOC=0\%}^{+}}{c_{s\_SOC=100\%}^{-} - c_{s\_SOC=0\%}^{-}} \\ \quad \times (c_{s\_mean}^{-} - c_{s\_SOC=0\%}^{-}) + c_{s\_SOC=0\%}^{+} \\ = K(c_{s\_mean}^{-} - c_{s\_SOC=0\%}^{-}) + c_{s\_SOC=0\%}^{+} \\ K = \frac{c_{s\_SOC=100\%}^{+} - c_{s\_SOC=0\%}^{+}}{c_{s\_SOC=100\%}^{-} - c_{s\_SOC=0\%}^{-}} \end{cases} \quad (25)$$

The relationship between the mean lithium-ion concentrations of positive and negative electrodes before and after correction can be obtained from (25) as

$$\begin{cases} c_{s\_mean}^{+}(k + 1) = K(c_{s\_mean}^{-}(k + 1) - c_{s\_SOC=0\%}^{-}) \\ \quad + c_{s\_SOC=0\%}^{+} \\ c_{s\_mean}^{+*}(k + 1) = K(c_{s\_mean}^{-*}(k + 1) - c_{s\_SOC=0\%}^{-}) \\ \quad + c_{s\_SOC=0\%}^{+} \end{cases} \quad (26)$$

By substituting (18) and (20) into (26), the relationship between  $\Delta c_{s\_mean}^{+}(k + 1)$  and  $\Delta c_{s\_mean}^{-}(k + 1)$  can be obtained as

$$\Delta c_{s\_mean}^{+}(k + 1) = K \Delta c_{s\_mean}^{-}(k + 1) \quad (27)$$

Substituting (19) and (21) into (27), one can obtain the relationship between  $\Delta c_s^{+}(k + 1)$  and  $\Delta c_s^{-}(k + 1)$  as

$$\Delta c_s^{+}(k + 1) = K \Delta c_s^{-}(k + 1) \quad (28)$$

## B. NERNST EQUATION FOR CORRECTING LITHIUM-ION CONCENTRATIONS

Although the relationship between the model output voltage and lithium-ion concentrations can be expressed in (16), it is difficult to directly deduce the corrected amount of lithium-ion concentrations according to the voltage error and (16). To address this issue, the Nernst equation is employed

in this work for computing and correcting the lithium-ion concentrations.

The Nernst equation describes the quantitative relationship between the standard electrode potential, activity of reactants, and the reversible potential of cell electrode. It is a concrete manifestation of thermodynamic equilibrium in the process of electrochemical reaction. For a chemical reaction shown as

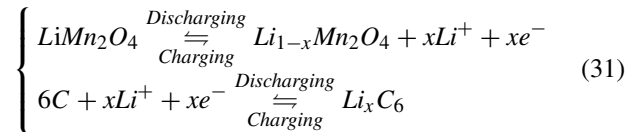


The electrode potential can be calculated by the Nernst equation as [35]

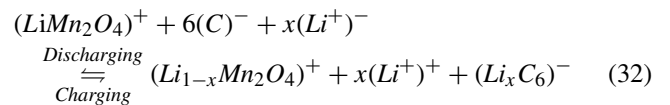
$$\varphi = \varphi^0 - \frac{RT}{nF} \ln \left( \frac{a(C)^c a(D)^d}{a(A)a(B)^b} \right) \quad (30)$$

where  $\varphi^0$  denotes the standard electrode potential,  $n$  represents the number of electrons transferred during the reaction, and  $a(\cdot)$  represents the activity of the counterpart.

The electrochemical reaction in the positive and negative electrodes of  $\text{LiMn}_2\text{O}_4$  batteries during the charging and discharging processes can be written as



The total electrochemical reactions in the battery can be expressed as



where  $(\cdot)^{+}$  and  $(\cdot)^{-}$  denote that the substance is in the positive and negative electrodes, respectively.

The electrode potential of the battery can be calculated by

$$\varphi = \varphi^0 - \frac{RT}{xF} \ln \frac{(a^{+}(\text{Li}^{+}))^x (a(\text{Li}_{1-x}\text{Mn}_2\text{O}_4))(a(\text{Li}_x\text{C}_6))}{(a^{-}(\text{Li}^{+}))^x (a(\text{LiMn}_2\text{O}_4))(a(\text{C}))^6} \quad (33)$$

where  $a^{+}(\text{Li}^{+})$  and  $a^{-}(\text{Li}^{+})$  represent the activity of  $\text{Li}^{+}$  in the positive and negative electrodes, respectively.

Since the solid activity is equal to 1, the electrode potential can be recalculated by

$$\varphi = \varphi^0 - \frac{RT}{xF} \ln \frac{(a^{+}(\text{Li}^{+}))^x}{(a^{-}(\text{Li}^{+}))^x} = \varphi^0 + \frac{RT}{F} \ln \frac{a^{-}(\text{Li}^{+})}{a^{+}(\text{Li}^{+})} \quad (34)$$

The degree of embedding is usually used to replace the activity, which refers to the ratio of the embedded quantity to the maximum embedded quantity in the current state [36]. In this paper, the embedded quantity of lithium ion is expressed by the mean lithium-ion concentration, and therefore, the relationship between the activity and concentration of lithium-ion can be defined by

$$\begin{cases} M = \frac{c_{s\_mean}}{c_{s,max}} \\ N = \frac{M}{1 - M} = \frac{c_{s\_mean}}{c_{s,max} - c_{s\_mean}} \end{cases} \quad (35)$$



where  $M$  denotes the degree of embedding, and  $N$  represents the activity.

The activity of  $\text{Li}^+$  in the positive and negative electrodes can be defined by

$$\begin{cases} N^+ = \frac{M^+}{1 - M^+} = \frac{c_{s,\text{mean}}^+}{c_{s,\text{max}}^+ - c_{s,\text{mean}}^+} \\ N^- = \frac{M^-}{1 - M^-} = \frac{c_{s,\text{mean}}^-}{c_{s,\text{max}}^- - c_{s,\text{mean}}^-} \end{cases} \quad (36)$$

where  $M^+$  and  $M^-$  denote the degrees of embedding, and  $N^+$  and  $N^-$  the activities of lithium-ion in positive and negative, respectively.

Substituting (36) into (34), one can express the electrode potential as

$$\varphi = \varphi^0 + \frac{RT}{F} \ln\left(\frac{c_{s,\text{mean}}^-}{c_{s,\text{max}}^- - c_{s,\text{mean}}^-} \frac{c_{s,\text{max}}^+ - c_{s,\text{mean}}^+}{c_{s,\text{mean}}^+}\right) \quad (37)$$

By substituting (37) into (15), the cell terminal voltage can be rewritten as

$$U(t) = \frac{RT}{F} \ln\left(\frac{c_{s,\text{mean}}^-(t)(c_{s,\text{max}}^+ - c_{s,\text{mean}}^+(t))}{c_{s,\text{mean}}^+(t)(c_{s,\text{max}}^- - c_{s,\text{mean}}^-(t))}\right) + \varphi^0 - I(t)R_c \quad (38)$$

By (38), the referenced cell terminal voltage and model output voltage at time instant  $k + 1$  can be calculated as

$$\begin{cases} U(k+1) = \frac{RT}{F} \ln\left(\frac{c_{s,\text{mean}}^-(k+1)(c_{s,\text{max}}^+ - c_{s,\text{mean}}^+(k+1))}{c_{s,\text{mean}}^+(k+1)(c_{s,\text{max}}^- - c_{s,\text{mean}}^-(k+1))}\right) \\ + \varphi^0 - I(t)R_c \\ U^*(k+1) = \frac{RT}{F} \ln\left(\frac{c_{s,\text{mean}}^{*-}(k+1)(c_{s,\text{max}}^+ - c_{s,\text{mean}}^{*+}(k+1))}{c_{s,\text{mean}}^{*+}(k+1)(c_{s,\text{max}}^- - c_{s,\text{mean}}^{*-}(k+1))}\right) \\ + \varphi^0 - I(t)R_c \end{cases} \quad (39)$$

To represent the difference between the  $c_{s,\text{max}}$  and  $c_{s,\text{mean}}$ , a variable  $D$  is defined as

$$\begin{cases} D^-(k+1) = c_{s,\text{max}}^- - c_{s,\text{mean}}^-(k+1) \\ D^+(k+1) = c_{s,\text{max}}^+ - c_{s,\text{mean}}^+(k+1) \end{cases} \quad (40)$$

Substituting (18), (20) and (40) into (39), one can obtain

$$\begin{cases} U(k+1) = \frac{RT}{F} \ln\left(\frac{c_{s,\text{mean}}^-(k+1)D^+(k+1)}{c_{s,\text{mean}}^+(k+1)D^-(k+1)}\right) \\ + \varphi^0 - I(t)R_c \\ U^*(k+1) = \frac{RT}{F} \ln\left(\frac{c_{s,\text{mean}}^-(k+1) + \Delta c_{s,\text{mean}}^-(k+1)}{c_{s,\text{mean}}^+(k+1) + \Delta c_{s,\text{mean}}^+(k+1)}\right) \\ + \frac{RT}{F} \ln\left(\frac{D^+(k+1) - \Delta c_{s,\text{mean}}^+(k+1)}{D^-(k+1) - \Delta c_{s,\text{mean}}^-(k+1)}\right) \\ + \varphi^0 - I(t)R_c \end{cases} \quad (41)$$

The voltage error ( $\Delta U$ ) between the referenced cell terminal voltage and model output voltage is determined by

$$\Delta U = U^*(k+1) - U(k+1) \quad (42)$$

Substituting (41) into (42), one can obtain

$$\begin{aligned} \Delta U = & \frac{RT}{F} \ln\left(\frac{c_{s,\text{mean}}^-(k+1) + \Delta c_{s,\text{mean}}^-(k+1)}{D^-(k+1) - \Delta c_{s,\text{mean}}^-(k+1)}\right) \\ & + \frac{RT}{F} \ln\left(\frac{D^+(k+1) - \Delta c_{s,\text{mean}}^+(k+1)}{c_{s,\text{mean}}^+(k+1) + \Delta c_{s,\text{mean}}^+(k+1)}\right) \\ & - \frac{RT}{F} \ln\left(\frac{c_{s,\text{mean}}^-(k+1)D^+(k+1)}{c_{s,\text{mean}}^+(k+1)D^-(k+1)}\right) \end{aligned} \quad (43)$$

Let

$$H = \frac{c_{s,\text{mean}}^-(k+1)}{D^-(k+1)} \frac{D^+(k+1)}{c_{s,\text{mean}}^+(k+1)} \exp\left(\Delta U \frac{F}{RT}\right) \quad (44)$$

Substituting (43) into (44) yields

$$H = \frac{c_{s,\text{mean}}^-(k+1) + \Delta c_{s,\text{mean}}^-(k+1)}{D^-(k+1) - \Delta c_{s,\text{mean}}^-(k+1)} \frac{D^+(k+1) - \Delta c_{s,\text{mean}}^+(k+1)}{c_{s,\text{mean}}^+(k+1) + \Delta c_{s,\text{mean}}^+(k+1)} \quad (45)$$

Substituting (27) into (45), one obtains

$$H = \frac{c_{s,\text{mean}}^-(k+1) + \Delta c_{s,\text{mean}}^-(k+1)}{D^-(k+1) - \Delta c_{s,\text{mean}}^-(k+1)} \frac{D^+(k+1) - K \Delta c_{s,\text{mean}}^-(k+1)}{c_{s,\text{mean}}^+(k+1) + K \Delta c_{s,\text{mean}}^-(k+1)} \quad (46)$$

Through a mathematical transformation, one obtains

$$\begin{cases} A(\Delta c_{s,\text{mean}}^-(k+1))^2 + B \Delta c_{s,\text{mean}}^-(k+1) = C \\ A = (1 - H)K \\ B = HKD^- - E c_{s,\text{mean}}^+(k+1) + K c_{s,\text{mean}}^-(k+1) - D^+ \\ C = D^+ c_{s,\text{mean}}^-(k+1) - HD^- c_{s,\text{mean}}^+(k+1) \end{cases} \quad (47)$$

Thus, the corrected amount of mean lithium-ion concentration in the negative electrode is governed by

$$\begin{aligned} \Delta c_{s,\text{mean}}^-(k+1) &= \begin{cases} \frac{C}{B}, & A = 0, B \neq 0 \\ -\frac{B + \sqrt{4AC + B^2}}{2A}, & A \neq 0, 4AC + B^2 > 0 \\ 0, & \text{Others} \end{cases} \end{aligned} \quad (48)$$

By substituting (48) into (21), the corrected amount of lithium-ion concentration in each layer of the negative electrode can be obtained as

$$\Delta c_s^-(k+1) = \frac{2(n_1 - 1)^2}{n_1(2n_1 - 1)} \Delta c_{s,\text{mean}}^-(k+1) \quad (49)$$

Substituting (49) into (28), one obtains the corrected amount of lithium-ion concentration in each layer of the positive electrode as

$$\Delta c_s^+(k+1) = \frac{2(n_1 - 1)^2}{n_1(2n_1 - 1)} K \Delta c_{s,\text{mean}}^-(k+1) \quad (50)$$

The scheme of the proposed SOC estimation method is shown in Fig. 3. The initial value of the battery model

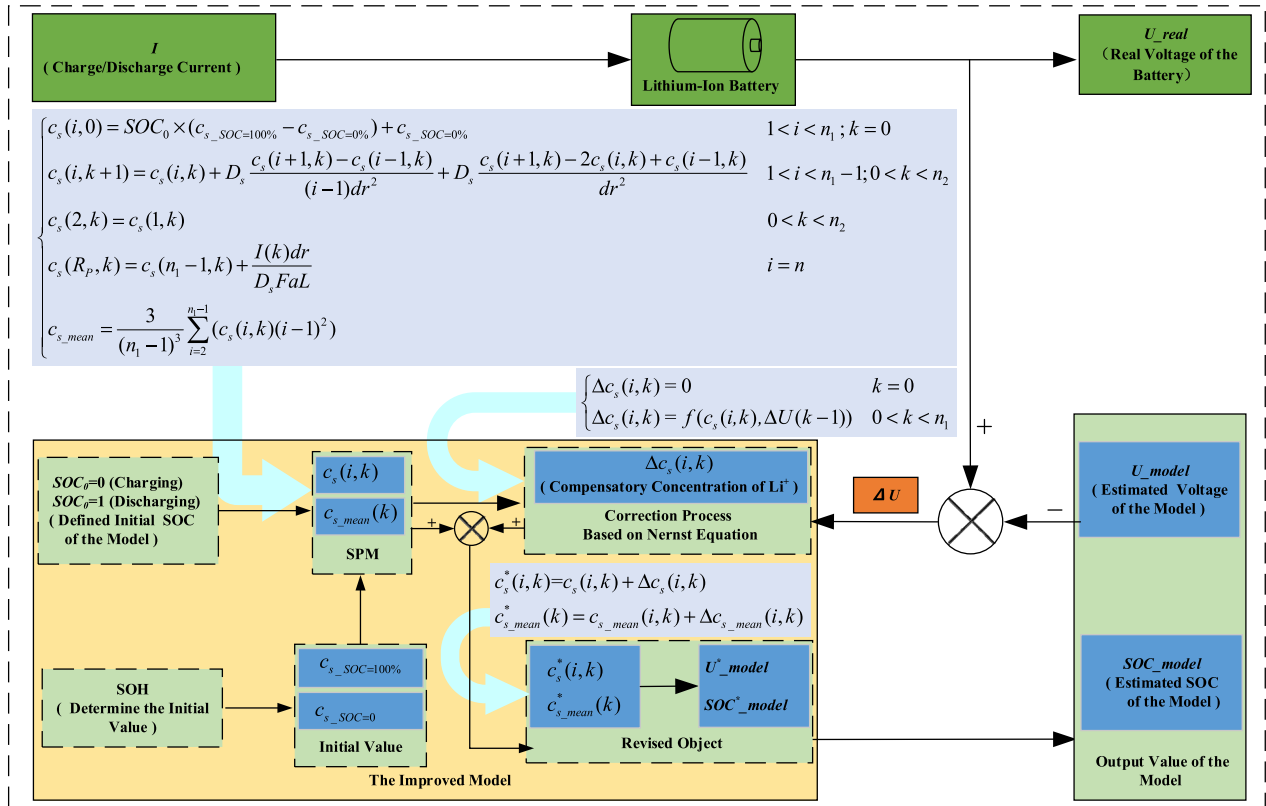


FIGURE 3. The scheme of the proposed SOC estimation method.

is given at the initial time instant,  $k = 0$ . The voltage error,  $\Delta U$ , between the battery terminal voltage and the model output voltage is fed back to the correction module that is deduced based on the Nernst equation for correcting lithium-ion concentrations at the next time instant. Then, the updated lithium-ion concentrations are used to compute the estimated SOC and model output voltage.

#### IV. EXPERIMENTAL RESULTS AND DISCUSSIONS

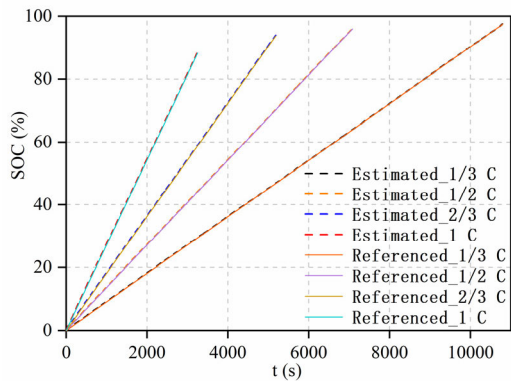
The LiMn<sub>2</sub>O<sub>4</sub> battery cells with the rated capacity of 90 Ah are employed in the battery experimental tests. Due to the limitation of present commercial battery techniques, some battery manufacturers suggest charging the battery with the current rate of less than 1 C (e.g., 1/3 C) to ensure the safety of battery systems. The current rate range from 1/3 C to 1 C is widely used in applications, literature, and some standard battery test manuals [4], [8], [20], [21], [37]–[39]. Thus, the experiments are mainly conducted at the current rate range from 1/3 C to 1 C. The test data, including the loading current, and charge or discharge capacity, are recorded by a battery charger and stored in a host computer. Specifically, the recorded charging and discharging capacities during the experiments are used to compute the battery’s referenced SOC that would be compared with the estimates.

To evaluate the performance of the proposed estimation method against different charging and discharging currents, the battery cell is loaded with eight various charging

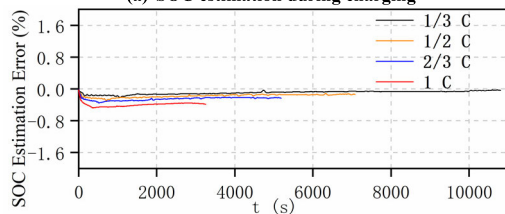
and discharge current rates including  $\pm 1/3 C$ ,  $\pm 1/2 C$ ,  $\pm 2/3 C$ , and  $\pm 1 C$ , and the test data are used for the verification.

Fig. 4 shows the SOC estimation results when the battery SOH is 100% and its initial SOC is 0% and 100% for the validations during the battery charging and discharging processes, respectively. The accurate initial SOC is given to the proposed model and algorithm. As shown in Fig. 4(a), although different current rates are applied to charge the battery, the SOC estimates can well track with the referenced SOC for each current rate. The SOC estimation errors between the estimates and references are depicted in Fig. 4(b), where the errors can be limited in a narrow band of  $\pm 0.50\%$ . The verification results during battery discharging processes are shown in Figs. 4(c) and 4(d). For different discharge current rates, promising SOC estimation results with the maximum absolute error of 0.8% can be achieved.

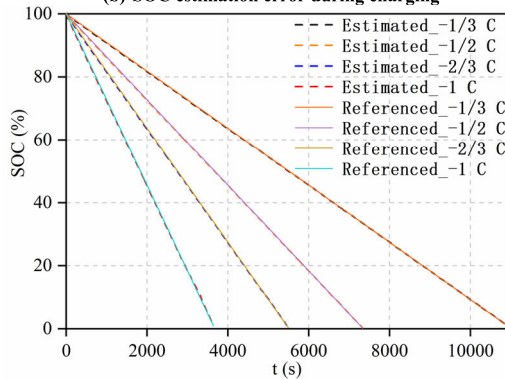
However, accurate initial battery SOC is usually unknown in real applications, especially after the battery has been in service for a long time. It is necessary to verify the proposed method in the case when the accurate initial SOC is unknown or an erroneous initial SOC is given. Herein, the battery charge and discharge experiments were carried out on batteries whose initial SOC is actually 50%, but set to 0% and 100% deliberately for battery charging and discharging processes, respectively, i.e. a 50% error of the initial SOC



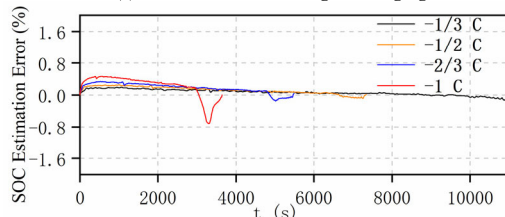
(a) SOC estimation during charging



(b) SOC estimation error during charging



(c) SOC estimation during discharging

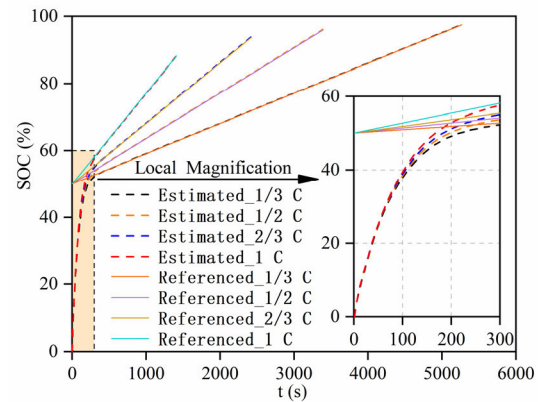


(d) SOC estimation error during discharging

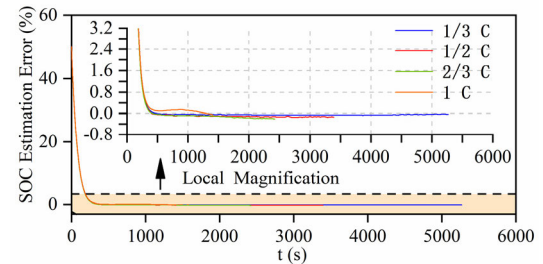
FIGURE 4. Battery SOC estimation results when given accurate initial SOC.

between the references and estimates. Fig.5 shows the SOC estimation results for this case.

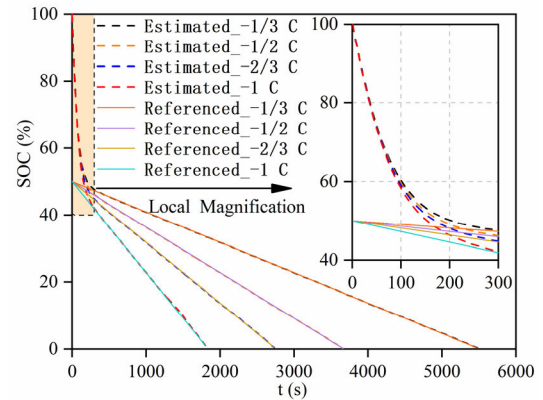
From Figs. 5(a) and 5(c), it can be found that in the early stage of charging or discharging processes, an initial SOC error of  $\pm 50\%$  can be observed. However, the estimates can quickly converge to their references, and then the estimated SOC keep on following the references closely. Figs. 5(b) and 5(d) show that in the first 250s, the SOC estimation errors significantly reduce from  $\pm 50\%$  to about  $\pm 1\%$ , and afterwards, the estimation errors can be maintained in an error band of  $\pm 0.8\%$ . Moreover, as shown in Figs. 5(d), a huge fluctuation of SOC estimation error at the end of



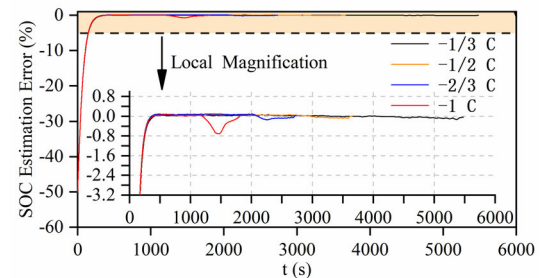
(a) SOC estimation during charging



(b) SOC estimation error during charging



(c) SOC estimation during discharging



(d) SOC estimation error during discharging

FIGURE 5. Battery SOC estimation results when given erroneous initial SOC.

battery discharging can be observed, especially at  $-1$  C. It is mainly caused by a massive change of battery polarization and ohmic resistance at high SOC [13], [40], [41], resulting in large SOC estimation errors at the end of battery discharging, especially at a high current rate. Fortunately,



the proposed algorithm can quickly correct this fluctuation and follow the tracks of the references. It is also worth mentioning that the value of this considerable fluctuation is still very small, about -0.8%, and it is acceptable within the allowable range of the error. The experimental results suggest that the proposed method can handle the case with erroneous initial SOC during both battery charging and discharging processes quite well.

To evaluate the robustness of the proposed method against varying cell aging, the proposed SOC estimation algorithm is validated with the test data of a battery cell degraded from 100% SOH to about 72% SOH. An erroneous initial SOC of 50% is always set to the model for the verification at different battery aging levels, and the estimation results are shown in Fig. 6.

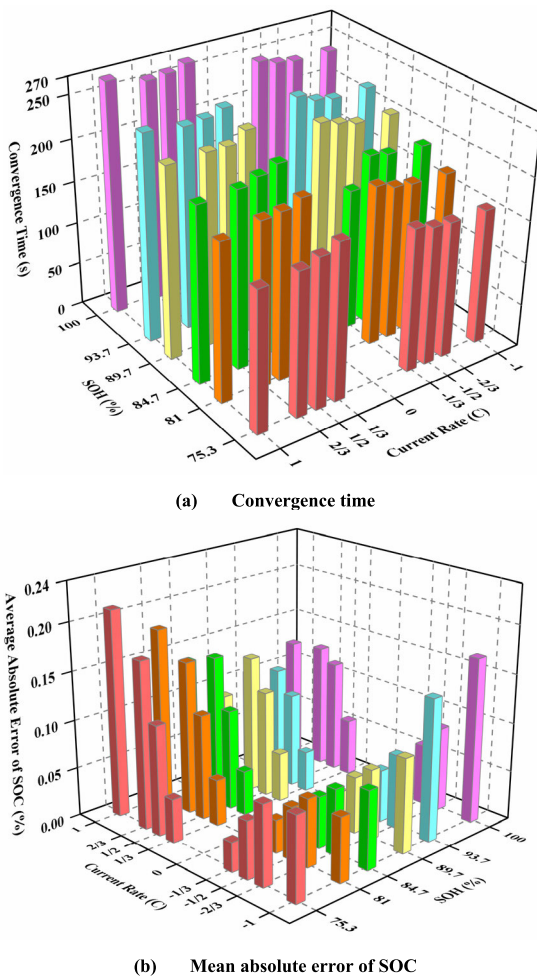


FIGURE 6. SOC estimation results at different cell aging levels.

As shown in Fig. 6(a), the convergence time, defined as the time period for the estimation error to reduce from its initial value to the range of  $\pm 1\%$ , is within 270s for batteries of different cell aging levels and loading current rates, which highlights the fast convergence rate of the proposed method. Regardless of the SOC estimation errors that occur before the convergence time, the mean absolute estimation errors are

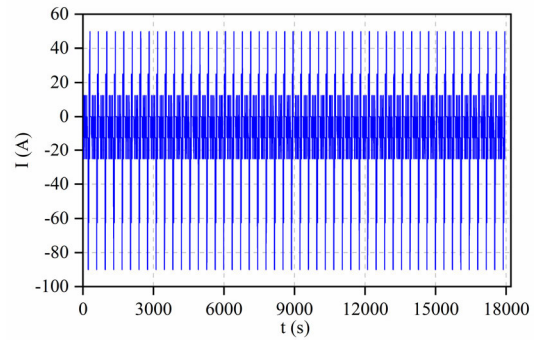


FIGURE 7. The Current profile of DST cycles.

depicted in Fig. 6(b). As shown, most of the mean absolute SOC estimation errors of less than 0.22% can be achieved at different cell aging levels with various loading current rates.

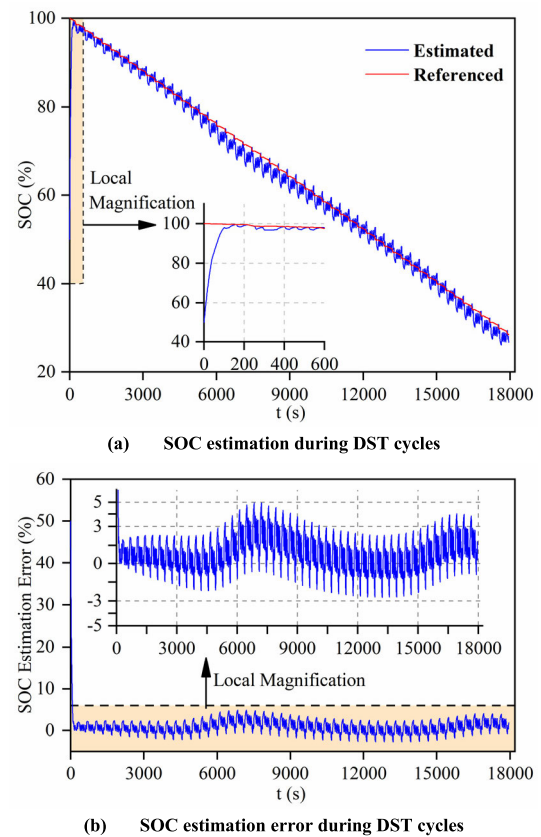


FIGURE 8. SOC estimation results during DST cycles.

Besides, to further verify the performance of the proposed method operating under dynamic loading conditions, the battery cell is tested with dynamic stress test (DST) cycles [38]. The current profile of DST cycles is depicted in Fig. 7, which has been widely used to mimic the actual battery operating currents, especially for electric vehicle applications. Before the execution of DST cycles, the battery cell is fully charged, and the referenced battery initial SOC is 100%. The model initial SOC is set to 50%, and the SOC estimation results during DST cycles are shown in Fig. 8. As shown in Fig. 8(a),

although there is a large initial SOC error applied to the proposed SOC estimation algorithm, the estimates can still converge to its references at about 100s and then follow the tracks of the references. The SOC estimation errors during DST cycles are depicted in Fig 8(b), wherein some error fluctuations can be observed, but specifically, most of the estimation errors can be confined within an error band of  $\pm 5.00\%$  with the mean absolute error of about 1.35%. It manifests that the proposed method for estimating battery SOC is still feasible under dynamic loading conditions.

**TABLE 2.** The comparison of the proposed method and other methods.

Ref.	Applied Estimation Technique	Different Aging is Considered?	Different Current Rate is Considered?	Mean Absolute Error (%)
[4]	PI Observer	No	No	<3%
[42]	Extended Kalman Filter	No	Yes	<4%
[43]	PDE Backstepping Observer	No	No	<0.2%
[44]	Extended Kalman Filter	No	No	<1%
[45]	Particle Filters	No	No	Unspecified
[46]	Nonlinear Robust Observers	No	No	<5%
This paper	Nernst Equation	Yes	Yes	<1.35%

The comparison between the proposed method and conventional EM-based methods reported in the references [4], [42]–[46] in terms of estimation absolute error and considering the influence factors of SOC estimation, such as cell aging and current rate, is listed in Table 2. It can be found that the EM-based methods with different observer/filter techniques can achieve accurate estimates. However, most reported techniques have not been evaluated under different operating conditions, such as various cell aging levels and loading current rates. The performance of proposed method in this paper has been systemically evaluated under different operating conditions, which indicates its high degree of robustness.

## V. CONCLUSION

In this paper, an approach based on a battery EM and the Nernst equation was proposed for estimating the SOC of lithium-ion batteries. A single particle model that reduces the complexity of typical battery EM while maintaining its capability to capture battery dynamics was employed in this work to provide a direct insight to compute the lithium-ion concentrations in solid particles. The voltage error between the cell referenced terminal voltage and model output voltage was used to correct the lithium-ion concentrations through a simple voltage negative feedback module. The corrected amount of lithium-ion concentration was

quantitatively deduced by the Nernst equation. The performance of the proposed method has been validated under different operating conditions, including various charging and discharging current rates, erroneous initial SOC, and cell aging levels. Experimental results showed that although an erroneous initial SOC of 50% was applied to the proposed algorithm, promising estimates with the mean absolute errors less than 1.35% could be still achieved for both constant and dynamic loading conditions, demonstrating the high degree robustness and effectiveness of the proposed SOC estimation method.

However, the practical application of EM-based methods is still impeded by their complexity, especially for embedded battery management systems with limited computational resources. Fortunately, the development of the cloud computing technique has great potential to address this issue. With the vast computational resources, the cloud computing technique can handle complicated EM-based algorithms with ease in real-time. Besides, most available solutions for estimating battery SOC were validated on a battery cell level. How to develop the SOC estimation method from a cell level to a pack level is still an open question. These tasks will be investigated in our future work.

## REFERENCES

- [1] N. A. Chaturvedi, R. Klein, J. Christensen, J. Ahmed, and A. Kojic, "Algorithms for advanced battery-management systems," *IEEE Control Syst. Mag.*, vol. 30, no. 3, pp. 49–68, Jun. 2010, doi: [10.1109/MCS.2010.936293](https://doi.org/10.1109/MCS.2010.936293).
- [2] Y. Zheng, Y. Lu, W. Gao, X. Han, X. Feng, and M. Ouyang, "Micro-short-circuit cell fault identification method for lithium-ion battery packs based on the mutual information," *IEEE Trans. Ind. Electron.*, early access, Apr. 9, 2020, doi: [10.1109/TIE.2020.2984441](https://doi.org/10.1109/TIE.2020.2984441).
- [3] W. Gao, Y. Zheng, M. Ouyang, J. Li, X. Lai, and X. Hu, "Micro-short-circuit diagnosis for series-connected lithium-ion battery packs using mean-difference model," *IEEE Trans. Ind. Electron.*, vol. 66, no. 3, pp. 2132–2142, Mar. 2019, doi: [10.1109/TIE.2018.2838109](https://doi.org/10.1109/TIE.2018.2838109).
- [4] L. Zheng, L. Zhang, J. Zhu, G. Wang, and J. Jiang, "Co-estimation of state-of-charge, capacity and resistance for lithium-ion batteries based on a high-fidelity electrochemical model," *Appl. Energy*, vol. 180, pp. 424–434, Oct. 2016, doi: [10.1016/j.apenergy.2016.08.016](https://doi.org/10.1016/j.apenergy.2016.08.016).
- [5] M. Uno and A. Kukita, "Cycle life evaluation based on accelerated aging testing for lithium-ion capacitors as alternative to rechargeable batteries," *IEEE Trans. Ind. Electron.*, vol. 63, no. 3, pp. 1607–1617, Mar. 2016, doi: [10.1109/TIE.2015.2504578](https://doi.org/10.1109/TIE.2015.2504578).
- [6] M. Ye, X. Song, R. Xiong, and F. Sun, "A novel dynamic performance analysis and evaluation model of series-parallel connected battery pack for electric vehicles," *IEEE Access*, vol. 7, pp. 14256–14265, 2019, doi: [10.1109/ACCESS.2019.2892394](https://doi.org/10.1109/ACCESS.2019.2892394).
- [7] X. Tang, C. Zou, T. Wik, K. Yao, Y. Xia, Y. Wang, D. Yang, and F. Gao, "Run-to-Run control for active balancing of lithium iron phosphate battery packs," *IEEE Trans. Power Electron.*, vol. 35, no. 2, pp. 1499–1512, Feb. 2020, doi: [10.1109/TPEL.2019.2919709](https://doi.org/10.1109/TPEL.2019.2919709).
- [8] K. Zhang, J. Ma, X. Zhao, D. Zhang, and Y. He, "State of charge estimation for lithium battery based on adaptively weighting cubature particle filter," *IEEE Access*, vol. 7, pp. 166657–166666, 2019, doi: [10.1109/ACCESS.2019.2953478](https://doi.org/10.1109/ACCESS.2019.2953478).
- [9] W. Wang and J. Mu, "State of charge estimation for lithium-ion battery in electric vehicle based on Kalman filter considering model error," *IEEE Access*, vol. 7, pp. 29223–29235, 2019, doi: [10.1109/ACCESS.2019.2895377](https://doi.org/10.1109/ACCESS.2019.2895377).
- [10] S. Peng, C. Chen, H. Shi, and Z. Yao, "State of charge estimation of battery energy storage systems based on adaptive unscented Kalman filter with a noise statistics estimator," *IEEE Access*, vol. 5, pp. 13202–13212, 2017, doi: [10.1109/ACCESS.2017.2725301](https://doi.org/10.1109/ACCESS.2017.2725301).

- [11] V. Sangwan, R. Kumar, and A. Kumar Rathore, "State-of-charge estimation of li-ion battery at different temperatures using particle filter," *J. Eng.*, vol. 2019, no. 18, pp. 5320–5324, Jul. 2019, doi: [10.1049/joe.2018.9234](https://doi.org/10.1049/joe.2018.9234).
- [12] G. Dong, Z. Chen, J. Wei, and Q. Ling, "Battery health prognosis using brownian motion modeling and particle filtering," *IEEE Trans. Ind. Electron.*, vol. 65, no. 11, pp. 8646–8655, Nov. 2018, doi: [10.1109/TIE.2018.2813964](https://doi.org/10.1109/TIE.2018.2813964).
- [13] L. Zheng, J. Zhu, G. Wang, D. D.-C. Lu, P. McLean, and T. He, "Experimental analysis and modeling of temperature dependence of lithium-ion battery direct current resistance for power capability prediction," in *Proc. 20th Int. Conf. Electr. Mach. Syst. (ICEMS)*, Aug. 2017, pp. 1–4.
- [14] X. Feng, C. Weng, X. He, X. Han, L. Lu, D. Ren, and M. Ouyang, "Online state-of-health estimation for li-ion battery using partial charging segment based on support vector machine," *IEEE Trans. Veh. Technol.*, vol. 68, no. 9, pp. 8583–8592, Sep. 2019, doi: [10.1109/TVT.2019.2927120](https://doi.org/10.1109/TVT.2019.2927120).
- [15] H. Karlsen, T. Dong, Z. Yang, and R. Carvalho, "Temperature-dependence in battery management systems for electric vehicles: Challenges, criteria, and solutions," *IEEE Access*, vol. 7, pp. 142203–142213, 2019, doi: [10.1109/ACCESS.2019.2943558](https://doi.org/10.1109/ACCESS.2019.2943558).
- [16] M. Ye, H. Gong, R. Xiong, and H. Mu, "Research on the battery charging strategy with charging and temperature rising control awareness," *IEEE Access*, vol. 6, pp. 64193–64201, 2018, doi: [10.1109/ACCESS.2018.2876359](https://doi.org/10.1109/ACCESS.2018.2876359).
- [17] X. Kuang, K. Li, Y. Xie, C. Wu, P. Wang, X. Wang, and C. Fu, "Research on control strategy for a battery thermal management system for electric vehicles based on secondary loop cooling," *IEEE Access*, vol. 8, pp. 73475–73493, 2020, doi: [10.1109/ACCESS.2020.2986814](https://doi.org/10.1109/ACCESS.2020.2986814).
- [18] W. Huang, W. Zhang, A. Chen, Y. Zhang, and M. Li, "A co-simulation method based on coupled thermoelectric model for electrical and thermal behavior of the lithium-ion battery," *IEEE Access*, vol. 7, pp. 180727–180737, 2019, doi: [10.1109/ACCESS.2019.2958940](https://doi.org/10.1109/ACCESS.2019.2958940).
- [19] L. Zheng, J. Zhu, G. Wang, D. D.-C. Lu, and T. He, "Differential voltage analysis based state of charge estimation methods for lithium-ion batteries using extended Kalman filter and particle filter," *Energy*, vol. 158, pp. 1028–1037, Sep. 2018, doi: [10.1016/j.energy.2018.06.113](https://doi.org/10.1016/j.energy.2018.06.113).
- [20] Z. Liu, X. Dang, and B. Jing, "A novel open circuit voltage based state of charge estimation for lithium-ion battery by multi-innovation Kalman filter," *IEEE Access*, vol. 7, pp. 49432–49447, 2019, doi: [10.1109/ACCESS.2019.2910882](https://doi.org/10.1109/ACCESS.2019.2910882).
- [21] Y. Li, H. Guo, F. Qi, Z. Guo, and M. Li, "Comparative study of the influence of open circuit voltage tests on state of charge online estimation for lithium-ion batteries," *IEEE Access*, vol. 8, pp. 17535–17547, 2020, doi: [10.1109/ACCESS.2020.2967563](https://doi.org/10.1109/ACCESS.2020.2967563).
- [22] W. Waag and D. U. Sauer, "Adaptive estimation of the electromotive force of the lithium-ion battery after current interruption for an accurate state-of-charge and capacity determination," *Appl. Energy*, vol. 111, pp. 416–427, Nov. 2013, doi: [10.1016/j.apenergy.2013.05.001](https://doi.org/10.1016/j.apenergy.2013.05.001).
- [23] X. Tan, Y. Tan, D. Zhan, Z. Yu, Y. Fan, J. Qiu, and J. Li, "Real-time state-of-health estimation of lithium-ion batteries based on the equivalent internal resistance," *IEEE Access*, vol. 8, pp. 56811–56822, 2020, doi: [10.1109/ACCESS.2020.2979570](https://doi.org/10.1109/ACCESS.2020.2979570).
- [24] A. Cuadras and O. Kanoun, "SoC li-ion battery monitoring with impedance spectroscopy," in *Proc. 6th Int. Multi-Conf. Syst., Signals Devices*, Djerba, Tunisia, May 2009, pp. 1–5.
- [25] J. Lu, Z. Chen, Y. Yang, and M. L. V., "Online estimation of state of power for lithium-ion batteries in electric vehicles using genetic algorithm," *IEEE Access*, vol. 6, pp. 20868–20880, 2018, doi: [10.1109/ACCESS.2018.2824559](https://doi.org/10.1109/ACCESS.2018.2824559).
- [26] R. Karmakar and S. Chattopadhyay, "Window-based peak power model and particle swarm optimization guided 3-dimensional bin packing for SoC test scheduling," *Integration*, vol. 50, pp. 61–73, Jun. 2015, doi: [10.1016/j.vlsi.2015.01.006](https://doi.org/10.1016/j.vlsi.2015.01.006).
- [27] P. Singh, R. Vinjamuri, X. Wang, and D. Reisner, "Design and implementation of a fuzzy logic-based state-of-charge meter for li-ion batteries used in portable defibrillators," *J. Power Sources*, vol. 162, no. 2, pp. 829–836, Nov. 2006, doi: [10.1016/j.jpowsour.2005.04.039](https://doi.org/10.1016/j.jpowsour.2005.04.039).
- [28] F. Zhang, T.-Y. Wu, Y. Wang, R. Xiong, G. Ding, P. Mei, and L. Liu, "Application of quantum genetic optimization of LVQ neural network in smart city traffic network prediction," *IEEE Access*, vol. 8, pp. 104555–104564, 2020, doi: [10.1109/ACCESS.2020.2999608](https://doi.org/10.1109/ACCESS.2020.2999608).
- [29] O. Ojo, H. Lang, Y. Kim, X. Hu, B. Mu, and X. Lin, "A neural network-based method for thermal fault detection in lithium-ion batteries," *IEEE Trans. Ind. Electron.*, early access, Apr. 13, 2020, doi: [10.1109/TIE.2020.2984980](https://doi.org/10.1109/TIE.2020.2984980).
- [30] L. Zhang, K. Li, D. Du, C. Zhu, and M. Zheng, "A sparse least squares support vector machine used for SOC estimation of li-ion batteries," *IFAC-PapersOnLine*, vol. 52, no. 11, pp. 256–261, 2019, doi: [10.1016/j.ifacol.2019.09.150](https://doi.org/10.1016/j.ifacol.2019.09.150).
- [31] R. Xiong, J. Cao, Q. Yu, H. He, and F. Sun, "Critical review on the battery state of charge estimation methods for electric vehicles," *IEEE Access*, vol. 6, pp. 1832–1843, 2018, doi: [10.1109/ACCESS.2017.2780258](https://doi.org/10.1109/ACCESS.2017.2780258).
- [32] Q. Zhu, L. Li, X. Hu, N. Xiong, and G.-D. Hu, " $H_\infty$ -based nonlinear observer design for state of charge estimation of lithium-ion battery with polynomial parameters," *IEEE Trans. Veh. Technol.*, vol. 66, no. 12, pp. 10853–10865, Dec. 2017, doi: [10.1109/TVT.2017.2723522](https://doi.org/10.1109/TVT.2017.2723522).
- [33] K. Dai, J. Wang, and H. He, "An improved SOC estimator using time-varying discrete sliding mode observer," *IEEE Access*, vol. 7, pp. 115463–115472, 2019, doi: [10.1109/ACCESS.2019.2932507](https://doi.org/10.1109/ACCESS.2019.2932507).
- [34] B. Xiong, J. Zhao, Y. Su, Z. Wei, and M. Skyllas-Kazacos, "State of charge estimation of vanadium redox flow battery based on sliding mode observer and dynamic model including capacity fading factor," *IEEE Trans. Sustain. Energy*, vol. 8, no. 4, pp. 1658–1667, Oct. 2017, doi: [10.1109/TSTE.2017.2699288](https://doi.org/10.1109/TSTE.2017.2699288).
- [35] V. Dimitrov and L. Gorker, "Modified nernst equation for electroless metal deposition," *Prog. Reaction Kinetics Mechanism*, vol. 31, no. 1, pp. 45–58, Jan. 2006, doi: [10.3184/007967406779133957](https://doi.org/10.3184/007967406779133957).
- [36] C. Julien, A. Mauger, A. Vijn, and K. Zaghbi, *Lithium Batteries\_Science and Technology*, 2th ed. New York, NY, USA: Springer, 2016, pp. 69–91.
- [37] X. Cui, Z. Jing, M. Luo, Y. Guo, and H. Qiao, "A new method for state of charge estimation of lithium-ion batteries using square root cubature Kalman filter," *Energies*, vol. 11, no. 1, p. 209, Jan. 2018, doi: [10.3390/en11010209](https://doi.org/10.3390/en11010209).
- [38] *Electric Vehicle Battery Test Procedures Manual*, USABC and D.N.L. Personnel, Washington, DC, USA, 1996.
- [39] *Battery Technology Life Verification Test Manual*, Idaho Nat. Lab., Idaho Falls, ID, USA, 2005.
- [40] F. Maletic and J. Deur, "Analysis of ECM-based li-ion battery state and parameter estimation accuracy in the presence of OCV and polarization dynamics modeling errors," in *Proc. IEEE 29th Int. Symp. Ind. Electron. (ISIE)*, Jun. 2020, pp. 1318–1324.
- [41] Y. Bao, W. Dong, and D. Wang, "Online internal resistance measurement application in lithium ion battery capacity and state of charge estimation," *Energies*, vol. 11, no. 5, p. 1073, Apr. 2018, doi: [10.3390/en11051073](https://doi.org/10.3390/en11051073).
- [42] Y. Liu, Y. Huangfu, R. Ma, L. Xu, D. Zhao, and J. Wei, "State of charge estimation of lithium-ion batteries electrochemical model with extended Kalman filter," in *Proc. IEEE Ind. Appl. Soc. Annu. Meeting*, Sep. 2019, pp. 1–7.
- [43] S. Tang, Y. Wang, Z. Sahinoglu, T. Wada, S. Hara, and M. Krstic, "State-of-charge estimation for lithium-ion batteries via a coupled thermal-electrochemical model," in *Proc. Amer. Control Conf. (ACC)*, Jul. 2015, pp. 5871–5877.
- [44] R. Xiong, L. Li, and Q. Yu, "Improved single particle model based state of charge and capacity monitoring of lithium-ion batteries," in *Proc. IEEE 89th Veh. Technol. Conf. (VTC-Spring)*, Apr. 2019, pp. 1–5.
- [45] M. F. Samadi, S. M. M. Alavi, and M. Saif, "An electrochemical model-based particle filter approach for lithium-ion battery estimation," in *Proc. IEEE 51st IEEE Conf. Decis. Control (CDC)*, Dec. 2012, pp. 3074–3079.
- [46] S. Dey, B. Ayalew, and P. Pisu, "Nonlinear robust observers for state-of-charge estimation of lithium-ion cells based on a reduced electrochemical model," *IEEE Trans. Control Syst. Technol.*, vol. 23, no. 5, pp. 1935–1942, Sep. 2015, doi: [10.1109/TCST.2014.2382635](https://doi.org/10.1109/TCST.2014.2382635).

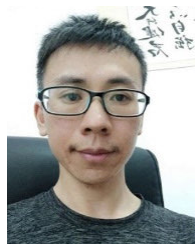


**LIHUA LIU** received the B.E. degree in engineering (electrical engineering and automation) from Tiangong University, Tianjin, China, in 2018, where she is currently pursuing the M.S. degree in electrical engineering. Her research interests include electrochemical characteristics of lithium-ion batteries and battery management.



**JIANGUO ZHU** (Senior Member, IEEE) received the B.E. degree in electrical engineering from the Jiangsu Institute of Technology, Jiangsu, China, in 1982, the M.E. degree in electrical engineering from the Shanghai University of Technology, Shanghai, China, in 1987, and the Ph.D. degree in electrical engineering from the University of Technology Sydney (UTS), Sydney, Australia, in 1995. He was appointed a Lecturer with UTS, in 1994, promoted to a Full Professor, in 2004, and a Distinguished Professor of electrical engineering, in 2017. At UTS, he has held various leadership positions, including the Head of the School for the School of Electrical, Mechanical and Mechatronic Systems, and the Director for Centre of Electrical Machines and Power Electronics. He joined The University of Sydney, Australia, as a Full Professor, in 2018, where he is currently the Head of the School for School of Electrical and Information Engineering. His research interests include computational electromagnetics, measurement and modeling of magnetic properties of materials, electrical machines and drives, power electronics, renewable energy systems, and smart micro grids.

His research interests include computational electromagnetics, measurement and modeling of magnetic properties of materials, electrical machines and drives, power electronics, renewable energy systems, and smart micro grids.



**LINFENG ZHENG** (Member, IEEE) received the B.E. and M.E. degrees in electrical engineering from Beijing Jiaotong University, China, in 2011 and 2014, respectively, and the Ph.D. degree in electrical engineering from the University of Technology Sydney, Sydney, NSW, Australia, in 2018.

He is currently an Associate Professor with the Institute of Rail Transportation. He is also with the International Energy College, Jinan University, China. His research interests include the development of lithium-ion battery management techniques for electric vehicles and battery second-used techniques for energy storage systems. He was a recipient of the 2018 Chinese Government Award for Outstanding Self-financed Students Abroad.

• • •